Long-Slotted Plate Connections for Enhancing the Robustness of Steel Gravity Systems against Column Loss: Preliminary Results

J. M. Weigand[1*], T. Thonstad[1], and A. A. Seamone[2]

[1]Research Structural Engineer, Engineering Laboratory, National Institute of Standards and Technology, 100 Bureau Drive, Gaithersburg, MD 20899-8611
[2]Undergraduate Research Fellow, Civil, Environmental and Architectural Engineering, University of Colorado Boulder, 1111 Engineering Drive, Boulder, CO 80309-0428
[*]Corresponding author. Tel: (301) 975-3302; E-mail: jonathan.weigand@nist.gov

ABSTRACT

Steel gravity frames are commonly used in United States building construction practice, but they are potentially vulnerable to disproportionate collapse under column loss, as has been shown by recent experimental and analytical studies. To overcome these vulnerabilities, a new type of connection has been developed. These "enhanced" gravity connections, which could be implemented in new or existing structures, incorporate long-slotted steel plates that are welded to the column and bolted to the top and bottom flanges of the beam. An experimental program designed to evaluate the influence of the key geometric factors on the coupled flexural-axial performance of these enhanced connections is underway. This paper presents selected results from the first block of the full experimental design: the behavior, failure mode, and key measured quantities from a set of eight tests conducted on replicate specimens with nominally identical geometry. Long-slotted plates were axially tested in a single-lapped bolted configuration under monotonic tensile loads, to characterize the behavior and failure mode of the components. The preliminary results show that the connection bolts maintain pretension while slipping within the slot, and do not lose appreciable pretension until bearing occurs. The results were highly repeatable; the coefficient of variation in the peak tensile load, and displacement at the peak tensile load was 0.025 and 0.032, respectively.

INTRODUCTION

Recent research has identified that steel gravity framing systems with conventional shear-tab connections are potentially vulnerable to disproportionate collapse under column loss scenarios. Four column removal tests performed on a half-scale steel gravity framing system with composite slab on steel deck showed that the floor system could only carry between 44 % and 62 % of the applicable gravity load combination [Johnson et al. 2015]. To help address this potential vulnerability, "enhanced" steel gravity connections that incorporate U-shaped top and seat plates, with long-slotted holes bolted to the beam flanges, have been developed. These enhanced connections could be implemented in new construction, or as a retrofit strategy for existing structures. The enhanced connections have been shown, using computational modeling, to provide more than double the resistance of the conventional shear-tab

connections [Weigand 2014; Weigand and Main 2016] when subjected to combined rotational and axial loads consistent with column removal. When implemented in system-level analyses of a two-bay by two-bay composite floor system, the enhanced connections increased the vertical load-carrying capacity of the system under center column loss by 90 % under static loading [Weigand and Main 2016]. These analyses also indicated that the system with the enhanced connections has the potential to resist the applicable gravity load combination under instantaneous dynamic center column loss. To begin developing a widely applicable design procedure, experimental validation and optimization of the U-shaped top and seat plates are needed.

This paper presents selected, preliminary results from an experimental program designed to evaluate the influence of geometric factors on the coupled flexural-axial performance of these enhanced connections. The intent of this research is to determine the optimal configuration of the slotted U-shaped plates for the range of anticipated connection configurations used in practice. Single-lapped long-slotted plate specimens were axially tested in a single-lapped bolted configuration under monotonic tensile loading, to-characterize their behavior and failure modes.

ENHANCED CONNECTIONS

An enhanced steel gravity connection is shown in Fig. 1. The connection includes a conventional shear-tab connection and top and seat plates, which are welded to the column and bolted to the beam flanges. Long-slotted holes in the top and seat plates permit large axial slip displacements of the flange bolts to occur prior to bearing at the ends of the slots. Rectangular plate washers distribute the bearing stresses induced by pre-tension in the flange bolts. The net section of the plate is designed relative to the shear area of the bolts to ensure significant plastic deformations are achieved in the plate and/or bolt prior to rupture, and can also be capacity-designed so that plate net tensile rupture over bolt shear rupture is the controlling failure mode. Standard holes are used in the beam flanges.

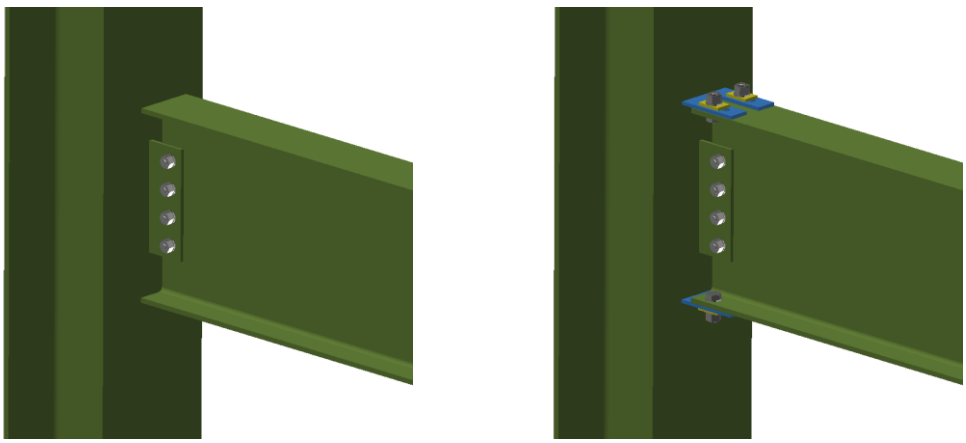

(a) (b)

Fig. 1. (a) Conventional single-plate shear connection, and (b) enhanced single-plate shear connection incorporating U-shaped slotted top and seat plates welded to column

COMPONENT TESTS

Component tests were performed to characterize the influence of the geometry of the top and seat plates on the coupled flexural-axial performance of the enhanced connection concept. The design of the component test specimens reduced the U-shaped top and seat plates down to their simplest possible component parts: representative widths of the top or seat plate with a long-slotted hole and beam-flange plates with a standard hole, as shown in Fig. 2. The two plates were connected by a single high-strength bolt. A 7.9 mm (5/16 in) thick plate washer covered the slot to distribute the bearing load induced by the bolt pretension over a larger area. To be as representative as possible of typical steel construction practices, the shear plates were fabricated from ASTM A36 steel [ASTM, 2014], while the beam-flange plates were fabricated from ASTM A572 Grade 50 steel [ASTM, 2018a]. By reducing the complexity of the test specimen, the influence of the geometric parameters of the components and the interactions between these parameters could be efficiently studied.

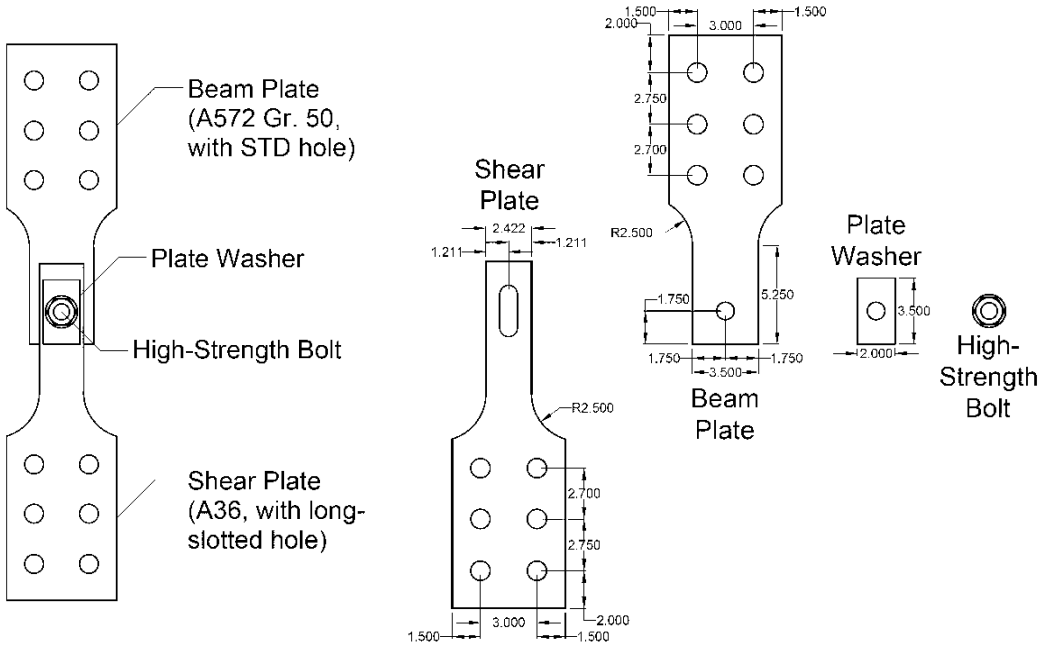

(a) (b)

Fig. 2: (a) typical steel component specimen, and (b) exploded view with annotated dimensions. All dimensions in inches, 1 in = 25.4 mm.

The design of experiments was based on a central composite rotatable design. The selected configurations were used to examine the influence of five aspects of the connection geometry, including the load ratio (i.e., the ratio of the bolt single-shear strength to the tensile rupture strength of the slotted plate), slot length ratio (i.e., slot length relative to the long-slot length (LSLT) in the Steel Construction Manual [AISC, 2017]), aspect ratio of the plate legs adjacent to the slot (width of leg to thickness of shear plate), bolt diameter, and bolt pretension ratio (i.e., ratio of the bolt pretension to $1.13T_{min}$, where $1.13T_{min}$ is the average installed bolt pretension, and T_{min} is the minimum bolt pretension specified in the Steel Construction Manual [AISC, 2017]). This paper presents selected results from the first block of the full

experimental design: the behavior, failure mode, and key measured quantities from a set of eight tests conducted on replicate specimens with nominally identical geometries (see Table 1).

Table 1: Specimen geometric parameters

Specimen ID	Bolt Diameter, mm (in)	Load Ratio	Slot Length Ratio	Bolt Pretension Ratio	Bolt Pretension kN (kip)	Aspect Ratio
SP001 SP002 SP003 SP004 SP005 SP006 SP007 SP008	22.2 (0.875)	1.10	1.25	1.00	196 (44.1)	1.50

The test protocol involved raising the upper fixture that holds the end of the beam plate, so that the lapped connection was placed under tensile loading. The tests were conducted in a self-reacting 1000 kN (220 kip) capacity servohydraulic load frame. The total expanded uncertainties in the measured actuator displacement and load were ±0.38 mm (0.015 in and ± 2.6 kN (0.6 kips), respectively. More information about how these uncertainties were evaluated is given in Appendix A. An impact wrench was used to tighten the six-bolt connections of the steel plates to the test fixtures to minimize any unanticipated displacements between the specimen and test fixtures during the tests. The specimen bolt was tightened by hand to the specified target pretension, measured using a load cell washer. The total expanded uncertainty in the measured bolt pretension was ±3.6 kN (0.8 kips). The tests were pseudo-static and were conducted in displacement control at a constant displacement rate of 2 mm/min (0.075 in/min).

The instrumentation for the component tests is shown schematically in Fig. 3b. Six potentiometers and four strain gauges were mounted on the specimens to measure relative displacements throughout the test rig and deformations within the specimen. These measurements were made to verify that the recorder displacements corresponded to deformations within the slotted connection region of the specimens. Four potentiometers were used to measure the slip between the test fixtures and the specimen, and two potentiometers were placed on either side of the bolted central connection. The total expanded uncertainty of these measurements was ±0.6 mm (0.02 in) (See Appendix A). The four strain gauges were placed on the side of the A36 slotted plate (two on each leg) to measure the deformation of the legs surrounding the slot. A load cell washer on the back side of the beam-flange plate allowed for the tension in the bolt to be measured directly.

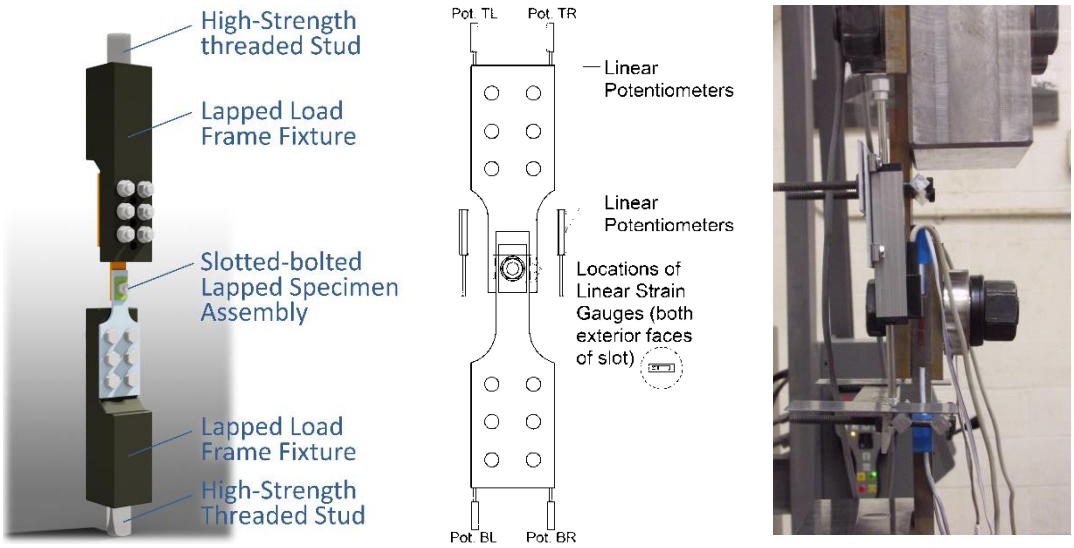

(a) (b) (c)

Fig. 3: (a) test configuration, and (b) instrumentation (c) instrumented specimen

OBSERVED RESULTS

Visible polishing of the surfaces of the lapped steel plates occurred during each test. These polished surfaces suggest that the coefficient of friction between the surfaces decreases throughout the test. Due to the inherent eccentricity in the lapped connection, significant bending of the two lapped plates and rotation of the connection bolt occurred once the bolt made contact and with the end of the slot, but not before. Each of the eight replicate specimens experienced bolt, rather than plate, rupture. This was anticipated, since a load ratio of greater than unity indicates that the plate strength was designed to be stronger than the bolt shear strength. The sheared bolts had a shiny crescent across the diameter of their cross-sections, as shown in Fig. 4. These shiny and dull lusters of the bolt rupture surface are attributable to slow, and fast fracture rates, respectively. Although standard procedures were used in applying the strain gauges, they did not remain attached throughout the entire test due to localized rotations occurring in the legs of the slotted shear plate. The strain gauges could typically only reach strains of 3 % to 4 % before becoming detached.

Fig. 4: shear rupture in bolt (SP005)

MEASURED RESULTS

Slip Displacements

The potentiometer measurements from the tests were used to verify that displacements in the test setup were concentrated within the lapped connection region of the specimen and minimized elsewhere. Fig. 5a shows the measured slip vs. actuator displacement for the four slip potentiometers for a typical test (see Fig. 3(b) for naming convention). Each potentiometer behaved similarly throughout the tests and did not reach a slip value of greater than 0.10 mm (0.0040 in) for any test. Given that the measured slips correspond to less than 0.3 % of the total deformation of the specimen at peak load, slip displacements were deemed negligible, and are subsequently ignored.

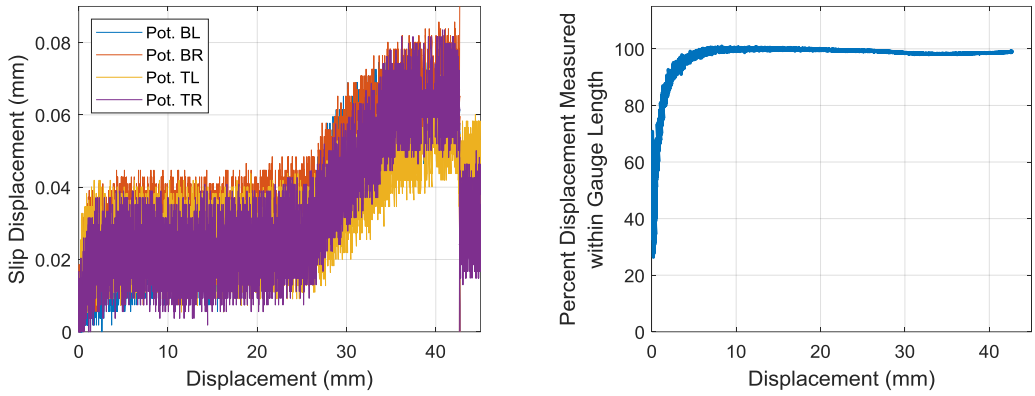

(a) (b)

Fig. 5: (a) slip displacements, and (b) percent displacement measured within gauge length

The total measured displacement, the sum of the slip deformation in the test setup and the deformation of the test specimen, was compared to the displacement measured by the hydraulic actuator's Linear Variable Differential Transformer (LVDT). Fig. 5(b) shows the ratio of the measured displacement within the lapped connection region to the actuator displacement as a percentage. This curve corresponds to the test with largest difference between the instrumentation and the actuator data. After the actuator displaced roughly 5 mm (0.2 in), the measured displacement within the lapped connection region was consistently within 1 % to 3 % of the measured actuator displacement. This is consistent with the negligible slip displacements measured between the test fixtures and the specimen. The good agreement between the actuator displacement and the displacement measurements gives confidence that the test configuration behaved as intended.

Force Displacement Response

Fig. 6 shows the typical force-displacement behavior of one of the tested specimens. Vertical lines designate four, distinct phases of the typical force-displacement response. Phase I represents the elastic portion of the connection response. This phase is typified by elastic deformations, with an initial stiffness of k_i, within the plates before

slipping of the bolt starts to occur along the slot. Phase II represents the bolt-slip portion of the response, during which the bolt travels along the length of the slot. The slope of the slip portion of the response is denoted as k_y. Phase III begins when the bolt has traveled the length of the slot and the bolt shaft comes into full bearing contact with both the end of the slot and the standard hole in the beam plate. This region is designated as the bearing stage of the connection response. The initial slope at the transition to Phase III is denoted as k_b. Phase IV begins after the specimen reaches its ultimate load, and failure of the connection begins to occur. The failure mode determines how abruptly the connection fails. Specimens that fail due to bolt shear, as was the case for the eight tested nominally identical specimens, lose strength abruptly, as demonstrated by Fig. 6.

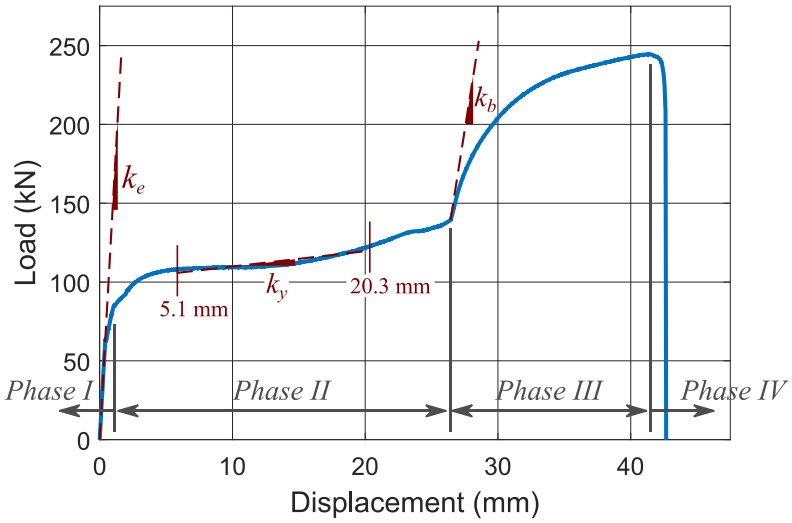

Fig. 6: Phases of the typical specimen load-displacement response

Bolt tension

A load cell washer was used to measure the pretension in the connection bolt throughout each test. The load in the load washer during testing of SP005 is shown in Fig. 7 along with the specimen's load-deformation response for context. The bolt maintained its pretension through the entire slip phase of the test and did not lose appreciable pretension (i.e. more than 15 %) until bearing occurred. Once the bolt came into bearing with the steel surface, the measured tension in the load cell washer decreased significantly; although some pretension remained in the bolt even at rupture.

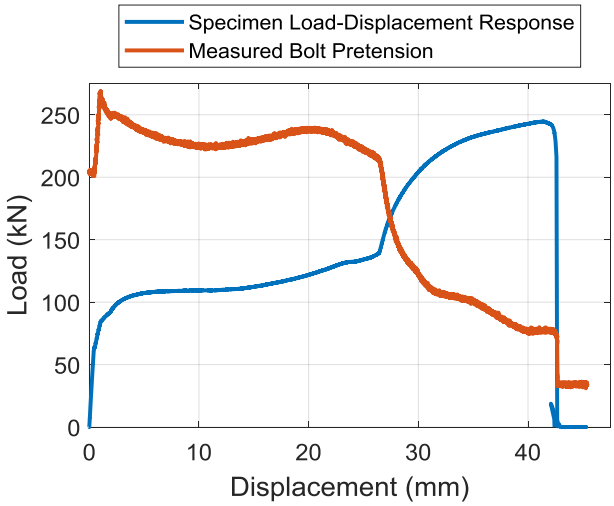

Fig. 7: Bolt tension versus displacement for SP005, which failed due to bolt shear rupture

VARIATION IN MEASURED RESPONSE

Table 2 shows key measured quantities of the force-displacement responses of the eight nominally identical test runs. The maximum force and its corresponding displacement are reported, along with the three stiffness values that characterize the shape of the load-displacement curve. The parameter, k_e, represents the initial elastic stiffness of the connection prior to slip (Phase I in Fig. 6); k_y, the average tangent slope of the slip region between 5.1 mm (0.20 in) and 20.3 mm (0.80 in); and k_b, the initial slope at initiation of bearing (beginning of Phase III).

Table 2: Center Point Test Data

			Stiffness Value		
Specimen ID	**Peak Load,**	**Displacement at Peak Load,**	k_e	k_y	k_b
	kN (kip)	mm (in)	kN/mm (kip/in)	kN/mm (kip/in)	kN/mm (kip/in)
SP001	265 (59.5)	38.1 (1.50)	147 650 (843.1)	1874 (10.7)	29 260 (167.1)
SP002	260 (58.5)	38.6 (1.52)	141 470 (807.8)	2644 (15.1)	33 480 (191.2)
SP003	256 (57.6)	40.6 (1.60)	135 600 (774.3)	1979 (11.3)	41 770 (238.5)
SP004	250 (56.1)	41.7 (1.64)	137 190 (783.4)	1944 (11.1)	36 430 (208.0)
SP005	245 (55.0)	41.4 (1.63)	134 460 (767.8)	1261 (7.2)	30 400 (173.6)
SP006	250 (56.1)	39.9 (1.57)	143 690 (820.5)	1594 (9.1)	23 940 (136.7)
SP007	250 (56.3)	41.7 (1.64)	131 030 (748.2)	1173 (6.7)	27 650 (157.9)
SP008	247 (55.6)	39.9 (1.57)	149 490 (853.6)	1716 (9.8)	44 590 (254.6)
Mean	253 (56.8)	40.1 (1.58)	140 070 (799.8)	1769 (10.1)	33 430 (190.9)
COV	0.025	0.032	0.044	0.244	0.199

At failure, the specimens with nominally identical geometries had a mean peak resistance of 253 kN (56.8 kip), with a coefficient of variation of 0.025. The small coefficient of variation in the ultimate load indicates that the results were highly

repeatable. The mean initial stiffness of the connection was 140 070 kN/mm (799.8 kip/in). This represents the elastic stiffness of the steel connection before slipping occurs. The mean stiffness of the slip response was 1769 kN/mm (10.1 kip/in). The mean initial stiffness of the bearing stage of the experiment was 33 430 kN/mm (190.9 kip/in). This represents the rate at which the connection reaches its maximum load before failure.

SUMMARY AND PRELIMINARY CONCLUSIONS

This paper presented selected results from an experimental program designed to characterize the influence of key geometric factors on the coupled flexural-axial performance of an enhanced connection concept for steel gravity framing systems. Long-slotted plates were axially tested in a single-lapped bolted configuration under monotonic loads to characterize the behavior and failure modes of the components.

From the component testing program, several preliminary conclusions can be drawn:

- Displacements in the test setup were concentrated within the lapped connection region of the specimen, as intended. Slip between the test fixtures and the specimen was negligible, accounting for less than 0.3 % of the measured displacement at the maximum force in each of the tests.

- Bolts maintained more than 85 % of their pretension through the entire slip phase of the tests. The bolts did not lose appreciable pretension until bearing occurred. Once the bolt shank came into bearing with the inner surfaces of the holes in the steel plates, the tension measured by the load cell washer decreased abruptly prior to specimen failure

- The tests were repeatable. Key measured quantities of the force-displacement responses of the eight nominally identical specimens were similar. The coefficient of variation (COV) for the maximum force was 0.025. The largest variations were in the post-slip and bearing stiffnesses: the COV for these measurements was 0.244 and 0.199, respectively.

DISCLAIMER

ACKNOWLEDGEMENTS

A portion of this work was performed by Andrew Seamone during his tenure as a NIST Summer Undergraduate Research Fellow (i.e., SURF student). The authors would like to thank the NIST SURF Program for supporting Mr. Seamone’s contribution to this work.

REFERENCES

AISC. (2011). Steel construction manual, 14 Ed., Chicago.

ASTM (2014). "Standard Specification for Carbon Structural Steel." Standard A36/A36M-14, ASTM International, West Conshohocken, PA.

ASTM (2018a), "Standard Specification for High-Strength Low-Alloy Columbium-Vanadium Structural Steel." Standard A572/A572M-18, ASTM International, West Conshohocken, PA.

Johnson, E.S. Meissner, and Fahnestock, L.A. (2015). "Experimental Behavior of a Half-Scale Steel Concrete Composite Floor System Subjected to Column Removal Scenarios." *Journal of Structural Engineering*, 04015133.

Taylor, B. N., and Kuyatt, C. E. (1994). "Guidelines for Evaluating and Expressing the Uncertainty of NIST Measurement Results." NIST Technical Note TN-1297, Gaithersburg, MD.

Weigand, J. M. and Main, J. W. (2016) "Enhanced Connections for Improved Robustness of Steel Gravity Frames." *Proc., Eighth International Workshop on Connections in Steel Structures (Connections VIII)*, Boston, Massachusetts, May 2016.

Weigand, J.M. (2014). "The Integrity of Steel Gravity Framing System Connections Subjected to Column Removal Loading." Ph.D. Dissertation in Civil Engineering, University of Washington, Seattle, WA.

APPENDIX A: UNCERTAINTY IN MEASUREMENTS

The measurements presented in this document include length (deformations and position) and force (applied load). For each measurement and instrument variety, Type A and/or Type B uncertainties, combined standard uncertainties, and total expanded uncertainties were estimated. As defined in Taylor and Kuyatt (1994), Type A uncertainty was evaluated using statistical methods; Type B uncertainty was estimated by other means such as the information available in manufacturer's specifications, from past-experience, or engineering judgement. The combined standard uncertainty was estimated by combining the individual uncertainties using "root-sum-of-squares" (Taylor and Kuyatt, 1994). The expended uncertainty was then computed by multiplying the combined uncertainty by a coverage factor of 2 corresponding to an approximately 95 % confidence interval.

Table A-1 summarizes the components of the measurement uncertainty. All uncertainties are assumed to be symmetric (+/-) and to have a Gaussian distribution.

Table A-1: Measurement Uncertainty

Measurement/Component	Type	Component Standard Uncertainty	Combined Standard Uncertainty	Total Expanded Uncertainty (k=2)
Actuator position				
Uncertainty in secondary standard	B	0.2 mm (0.006 in)	0.2 mm (0.007 in)	0.4 mm (0.015 in)
Uncertainty in calibration procedure (N=32)	A	0.2 mm (0.004 in)		
Actuator load				
Uncertainty in secondary standard	B	1.3 kN (0.3 kips)	1.3 kN (0.3 kips)	2.6 kN (0.6 kips)
Uncertainty in calibration procedure (N=32)	A	0.4 kN (0.1 kips)		
Load cell washer				
Uncertainty in secondary standard	B	1.3 kN (0.3 kips)	1.8 kN (0.4 kips)	3.6 kN (0.8 kips)
Uncertainty in calibration procedure (N=7)	A	1.3 kN (0.3 kips)		
Displacement Transducers				
Uncertainty in secondary standard (N=8)	A/B	2 µm (0.00006 in)	0.3 mm (0.01 in)	0.6 mm (0.02 in)
Uncertainty in calibration procedure (N=20)	A	0.3 mm (0.01 in)		